UNITED STATES DEPARTMENT OF THE INTERIOR

GEOLOGICAL SURVEY

Contour maps of uranium, uranium-thorium ratio, and total field magnetics, Lake City Area, San Juan Mountains, Colorado

Conducted and prepared by

High Life Helicopters Inc./QEB Inc

With an introduction by William D. Heran

U.S. Geological Survey

Open-File Report 81-568

1981

Introduction

by

William D. Heran

The data presented in this report is from an airborne high-sensitivity radiometric and magnetic survey conducted by High Life Helicopters, Inc. and its subsidiary QEB, Inc., for the U.S. Geological Survey. The area surveyed is located in the western San Juan Mountains, between Silverton and Lake City, Colorado. The general area covered is between 37°45′ and 38°07′30" latitude north and 107°15′ and 107°45′ longitude west (fig. A). Data collection was begun October 4, 1979 near Durango, Colorado and continued through October 8, 1979. Seventy-four north-south traverse lines were flown 400 feet above ground with a spacing of one-third mile and four east-west tie lines were flown at a spacing of 4 miles (Table A). The survey encompassed eleven 7.5 minute USGS topographic map sheets, and has a total of 786 line-miles of data (flight lines and corresponding topographic sheet names are shown on contour maps).

The survey was flown as part of a mineral appraisal study conducted in cooperation with the Bureau of Land Management (BLM). The survey was done to detect potential uranium mineralization and to better define the geology in the area.

This report is one of two open-file reports, and is accompanied by the contour maps for uranium, uranium-thorium ratio, and total field magnetics. The stacked profiles of all data, in microfische form, are available in U.S. Geological Survey Open File Report 81-567 (High Life Helicopters Inc./QEB Inc., with an introduction by W. D. Heran, 1981).

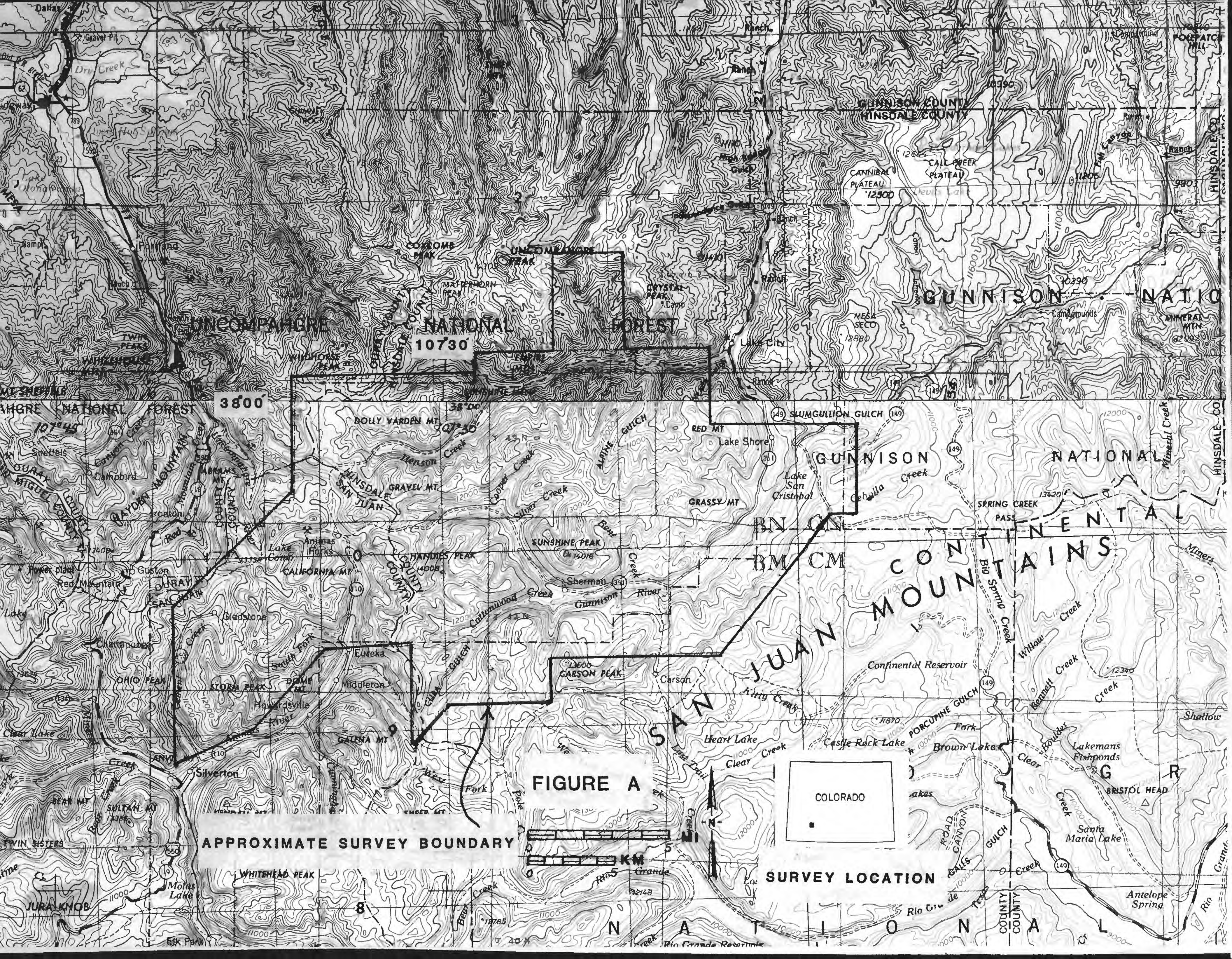

FIGURE A
APPROXIMATE SURVEY BOUNDARY
SURVEY LOCATION
COLORADO
MI
KM
N
10730'
3800'
UNCOMPAHGRE NATIONAL FOREST
GUNNISON NATIONAL FOREST
SAN JUAN MOUNTAINS
CONTINENTAL
GUNNISON COUNTY
HINSDALE COUNTY
Lake City
Silverton
Lake San Cristobal
SLUMGULLION GULCH
Continental Reservoir

Table A.--Flight line locations.

FLIGHT LINE NUMBER	BEGINNING		ENDING	
	LATITUDE NORTH (DEGREES)	LONGITUDE WEST (DEGREES)	LATITUDE NORTH (DEGREES)	LONGITUDE WEST (DEGREES)
1	37.9106	107.6897	37.8117	107.6917
2	37.9113	107.6842	37.8112	107.6858
3	37.9273	107.6783	37.8147	107.6794
4	37.9282	107.6711	37.8145	107.6717
5	37.9270	107.6689	37.8150	107.6667
6	37.9293	107.6603	37.8192	107.6592
7	37.9226	107.6536	37.8174	107.6550
8	37.9389	107.6475	37.8213	107.6489
9	37.9256	107.6414	37.8177	107.6422
10	37.9380	107.6350	37.8243	107.6336
11	37.9475	107.6294	37.8270	107.6303
12	37.9388	107.6239	37.8347	107.6283
13	37.9459	107.6175	37.8365	107.6186
14	37.9551	107.6119	37.8480	107.6122
15	37.9570	107.6056	37.8520	107.6061
16	37.9634	107.6006	37.8556	107.6014
17	38.0160	107.5936	37.8794	107.5947
18	38.0007	107.5886	37.8723	107.5878
19	38.0070	107.5808	37.8750	107.5803
20	38.0072	107.5753	37.8743	107.5747
21	38.0121	107.5689	37.8923	107.5675
22	38.0088	107.5631	37.8914	107.5636
23	38.9299	107.5575	37.8851	107.5572
23	38.0109	107.5575	37.9427	107.5633
24	38.0085	107.5506	37.8850	107.5511
25	38.0096	107.5436	37.8846	107.5461
26	38.0095	107.5372	37.8893	107.5383
27	38.0150	107.5331	37.8895	107.5339
28	38.0127	107.5258	37.8846	107.5269
29	38.0121	107.5208	37.8243	107.5203
30	38.0168	107.5150	37.9042	107.5156
30	37.8952	107.5142	37.8276	107.5142
31	38.0104	107.5081	37.8963	107.5078
31	37.8989	107.5042	37.8282	107.5089
32	38.0124	107.5017	37.8312	107.5019
33	38.0113	107.4964	37.8333	107.4986
34	38.0096	107.4900	37.8434	107.4889
35	38.0080	107.4839	37.8456	107.4836
36	38.0474	107.4764	37.8452	107.4775
37	38.0429	107.4717	37.8444	107.4714
38	38.0445	107.4658	37.8432	107.4656

Table A.--Flight line locations (continued)

FLIGHT LINE NUMBER	BEGINNING		ENDING	
	LATITUDE NORTH (DEGREES)	LONGITUDE WEST (DEGREES)	LATITUDE NORTH (DEGREES)	LONGITUDE WEST (DEGREES)
39	38.0434	107.4594	37.8465	107.4586
40	38.0424	107.4533	37.8418	107.4514
41	38.0472	107.4469	37.8464	107.4464
42	38.0424	107.4408	37.8433	107.4408
43	38.0667	107.4356	37.8426	107.4347
44	38.0671	107.4286	37.8469	107.4286
45	38.0775	107.4239	37.8591	107.4231
46	38.0729	107.4164	37.8590	107.4161
47	38.0756	107.4097	37.8562	107.4097
48	38.0737	107.4042	37.8623	107.4033
49	38.0736	107.3978	37.8634	107.3981
50	38.0727	107.3922	37.8622	107.3928
51	38.0710	107.3842	37.8555	107.3878
52	38.0681	107.3764	37.8606	107.3797
53	38.0487	107.3703	37.8771	107.3722
54	38.0428	107.3675	37.8561	107.3669
55	38.0477	107.3603	37.8594	107.3603
56	38.0442	107.3550	37.8573	107.3547
57	38.0433	107.3500	37.8567	107.3489
58	38.0393	107.3419	37.9708	107.3419
59	38.0199	107.3350	37.8768	107.3339
60	37.9920	107.3303	37.8781	107.3311
61	38.0064	107.3233	37.8834	107.3242
62	37.9953	107.3178	37.8945	107.3181
63	37.9961	107.3117	37.9011	107.3128
64	37.9958	107.3053	37.9058	107.3058
65	37.9498	107.2994	37.9065	107.3000
66	37.9515	107.2933	37.9154	107.2931
67	37.9495	107.2872	37.9218	107.2878
68	37.9899	107.2800	37.9232	107.2814
69	37.9936	107.2744	37.9336	107.2750
70	37.9957	107.2683	37.9408	107.2683
71	37.9943	107.2628	37.9278	107.2625
72	37.9971	107.2561	37.9435	107.2567
73	37.9949	107.2511	37.9392	107.2511
74	37.9906	107.2481	37.9352	107.2456
T1*	37.8770	107.6928	37.8736	107.3364
T2*	37.9423	107.6314	37.9341	107.2478
T3*	38.0026	107.5931	37.9820	107.2758
T4*	38.0367	107.4817	38.0389	107.3378

*east-west tie lines

General Discussion of Gamma Radiation and Instrumentation

The gamma radiation that is measured in an airborne survey includes background radiation and radiation originating within a thin layer at and beneath the ground surface. Soil, rock, and water effectively attenuate gamma radiation. Approximately 90 percent of the measured radiation, which originates beneath the ground surface, comes from the upper 0.3 m of soil or 0.7 m of water (Bailey and Childers, 1977).

The measuring unit consists of one or more crystals of thallium-activated sodium iodide, a material which emits a flash of light (scintillation), when hit by a gamma ray. The intensity of the scintillation is directly proportional to the energy of the gamma ray, which is a measurable function of the uranium, thorium, or potassium source. The scintillation is converted to a voltage, by a photomultiplier tube, and the pulse height is compared with that of a reference source. Voltage pulses are fed into separate diagnostic channels for uranium, thorium and radiopotassium and into a total-count channel. Output from each channel is then fed into a recorder as a count rate, which shows the number of gamma rays arriving per second within that particular energy range (Peters, 1978).

Gamma radiation that has energies sufficient to penetrate 100 to 200 m of air and be detected by a sodium-iodide crystal is given off by the decay of several isotopes of the uranium and thorium decay series, as well as of potassium. For aerial gamma-ray surveys, bismuth-214 is the important gamma emitter for the uranium series and thallium-208 is the important emitter for the thorium series. Uranium, thorium, and potassium gamma rays are high-energy photons (Adams and Gasparini, 1970) whose energies range from several KeV (thousand electron volts) to 2.8 MeV (million electron volts). The energies of the three important gamma rays, are 1.46 MeV (^{40}K) for potassium,

1.76 MeV (^{214}Bi) for uranium, and 2.62 MeV (^{208}Tl) for thorium.

Window spectrometers are used in most airborne surveys, and are designed with four windows to count photons that have the energies of interest. More sophisticated is the multichannel spectrometer that defines the full spectrum. A gamma-ray spectrometric survey has several advantages over total gamma radiation survey. First, uranium and thorium can be differentiated when both are present in significant amounts. Also, isotope-ratio maps can be produced from the data. Ground-surface configuration and other factors can produce weak anomalies in ^{214}Bi or ^{208}Tl, but the ratio of $^{214}Bi/^{208}Tl$ is only affected by real differences in one isotope relative to the other when elevation variations are corrected (Bailey and Childers, 1977).

General Geology

The survey area is located in the San Juan volcanic field in the San Juan Mountains in southwestern Colorado (fig. A). In general, the area is comprised of a Precambrian terrane covered in part by the extensive development of Tertiary volcanic units. Some Paleozoic rocks occur within the survey area but no Mesozoic rocks are recognized. A general geologic description of the San Juan volcanic field has been described by Lipman, Steven, and Mehnert (1970) and is outlined only briefly here.

The San Juan Mountains are an eroded volcanic plateau that form the largest remnant of a major composite middle-Tertiary volcanic field. In late Eocene or early Oligocene time, volcanic activity from many scattered stratovolcanoes produced a composite volcanic field covering more than 25,000 km^2 (Steven and Lipman, 1976). Early rocks are intermediate composition lavas and breccias, followed by silicic ash-flow tuff, and later by a bimodal association of basalt and alkali rhyolite.

About 30 m.y. ago volcanic activity changed to predominantly pyroclastic

eruptions, and large volume quartz latitic and rhyolitic ash flows. Approximately 25 m.y. ago, the character of erupted material changed to primarily basaltic material and some associated high-silica alkali-rich rhyolite. Basaltic eruptions continued intermittently until about 5 m.y. ago. During this time period, continued eruptions, local subsidence and caldera collapse resulted in the formation of 15 known calderas.

The western San Juan Mountains have a complex history of mineralization with several distinct periods of ore deposition extending over an interval of about 15 m.y. in later Tertiary time (Lipman and others, 1976). Only about one third of the calderas in the San Juan volcanic field are significantly mineralized (Steven, Luedke, and others, 1974). These calderas all had complex post subsidence histories including recurrent intrusion and extrusion of magma along the ring-fracture zones and related grabens (fig. B) (Steven and Lipman, 1976).

The western San Juan Mountains area is one of the richest and most intensely mineralized regions in the southern Rocky Mountains. This area has produced more than three-quarters of a billion dollars worth of base and precious metals during the last 100 years (Lipman and others, 1976). Ore deposits generally are associated with caldera and other volcanic structural features, with mineralization fracture controlled in breccia pipes, also as carbonate replacement, and disseminated in various host rock.

The primary function of calderas in mineralization thus appears to be the preparation of zones of weakness in the roofs of major magma chambers. If conditions at depth are favorable, some of these zones are the sites of recurrent igneous intrusions and extrusions, locally accompanied by hydrothermal activity and mineralization (Steven and Lipman, 1976).

This survey is concerned mainly with the location of uranium

mineralization in the area. To date there has been no mining of economic uranium deposits in the survey area, although some small prospects are known. The geologic environment is favorable for the occurrence of uranium mineralization, and further exploration is necessary.

Following this introduction, is a report prepared by High Life Helicopters Inc./QEB Inc. for the U.S. Geological Survey. This report is accompanied by the contour maps (total of 33) for uranium, uranium-thorium ratio, and total field magnetics. (Maps are labeled plates 1 thru 11 A, B, C; A series is uranium, B series is uranium-thorium ratio, C series is total field magnetics.) The maps also show the location of flight lines and fiducial points, and the corresponding U.S. Geological Survey 7 1/2 minute topographic sheet name.

PLATE 1 WETTERHORN PEAK QUADRANGLE
PLATE 2 UNCOMPAHGRE PEAK QUADRANGLE
PLATE 3 LAKE CITY QUADRANGLE
PLATE 4 IRONTON QUADRANGLE
PLATE 5 HANDIES PEAK QUADRANGLE
PLATE 6 REDCLOUD PEAK QUADRANGLE
PLATE 7 LAKE SAN CHRISTOBAL QUADRANGLE
PLATE 8 SILVERTON QUADRANGLE
PLATE 9 HOWARDSVILLE QUADRANGLE
PLATE 10 POLE CREEK MTN QUADRANGLE
PLATE 11 FINGER MESA QUADRANGLE

The stacked profiles of all data (in microfische form) are available in U.S. Geological Survey Open File Report 80-567. (High Life Helicopters Inc./QEB Inc. with an introduction by W. D. Heran, 1981).

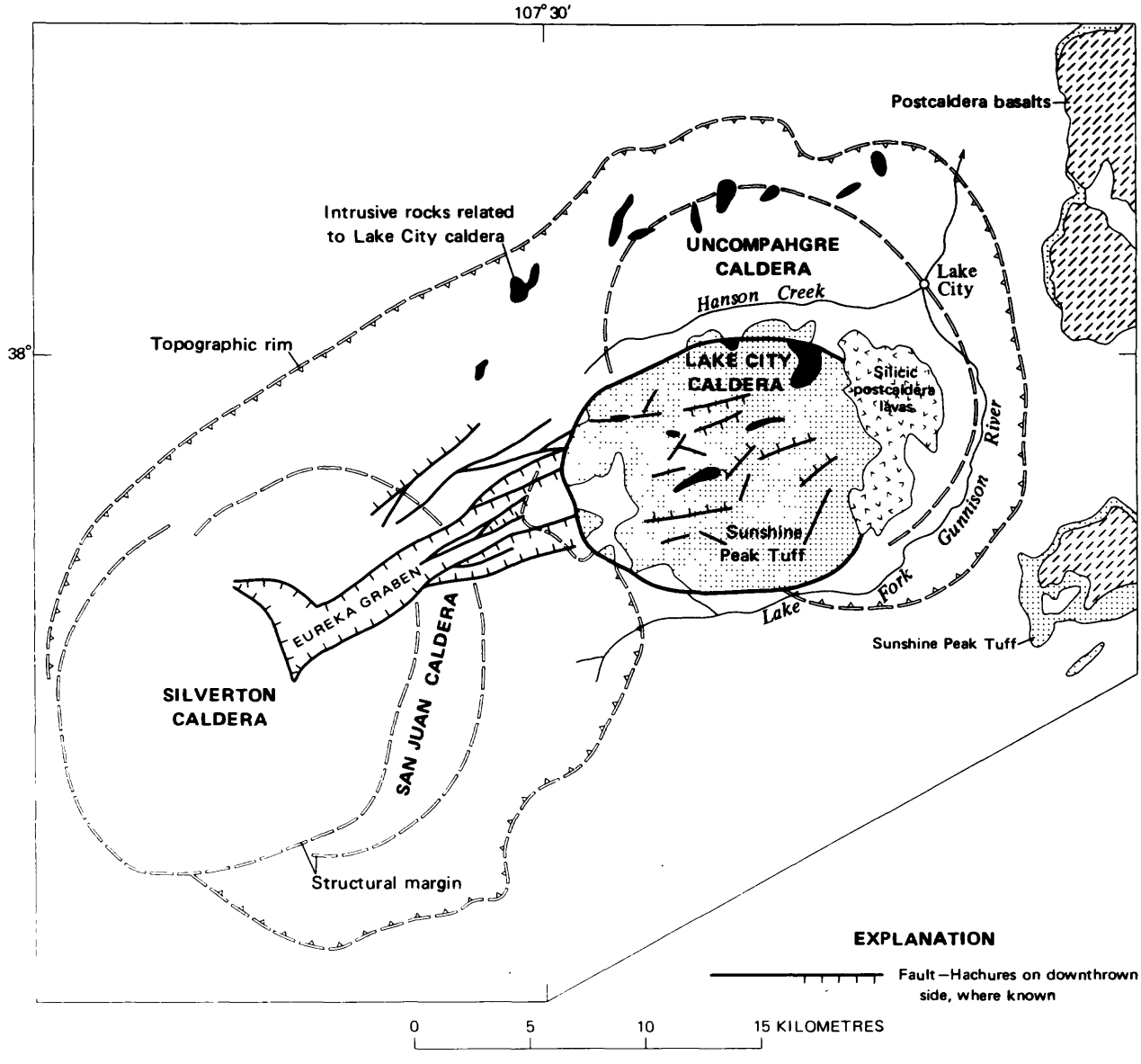

FIGURE B Generalized geologic map of San Juan caldera complex showing distribution of rocks related to the Lake City caldera (from Steven and Lipman, 1976).

References

Adams, J. A. S., and Gasparini, 1970, Gamma-ray spectrometry of rocks: Amsterdam, Elsevier, 295 p.

Bailey, R. V. and Childers, M. O., 1977, Applied mineral exploration with special reference to uranium: Westview Press, 513 p.

High Life Helicopters Inc./QEB Inc., With an introduction by W. D. Heran, 1981, Stacked profiles of data from a helicopter airborne radiometric and magnetic survey of the Lake City Area, San Juan Mountains, Colo.: U.S. Geological Survey Open-File Report 81-567.

Lipman, P. W., 1976, Geologic map of the Lake City caldera area, western San Juan Mountains, southwestern Colorado: U.S. Geological Survey Miscellaneous Investigations Series Map I-962.

Lipman, P. W., Steven, T. A., and Mehnert, H. H., 1970, Volcanic history of the San Juan Mountains, Colorado, as indicated by potassium-argon dating: Geological Society America Bulletin, v. 81, no. 8, p. 2329-2352.

Lipman, P. W., Steven, T. A., Luedke, R. G., and Burbank, W. S., 1973, Revised volcanic history of the San Juan, Uncompahgre, Silverton, and Lake City calderas in the western San Juan Mountains, Colorado: U.S. Geological Survey Journal of Research, v. 1., no. 6, p. 627-642.

Lipman, P. W., Fisher, F. S., Mehnert, H. H., Naeser, C. W., Luedke, R. G., and Steven, T. A., 1976, Multiple ages of mid-Tertiary mineralization and alteration in western San Juan Mountains, Colorado: Econ. Geology.

Peters, W. C., 1978, Exploration and Mining Geology, Chap. 13, p. 377.

Saunders, D. F. and Potts, 1978, Manual for the Application of NURE 1974-1977 Aerial Gamma-Ray Spectometer Data, Bendix Field Engineering Corp., U.S. Dept. of Energy Open-file Report 67BX-13(78).

Steven, T. A., and Lipman, P. W., Calderas of the San Juan Volcanic Field, southwestern Colorado, U.S. Geological Survey Professional Paper 958, 1976 p. 1-35.

Steven, T. A., and Luedke, R. G. and Lipman, P. W., 1974, Relation of mineralization to calderas in the San Juan volcanic field, southwestern Colorado: U.S. Geological Survey Journal of Research, v. 2., no. 4, p. 405-409.

Report by High Life Helicopters Inc/QEB Inc*

*The material in this report is the sole responsibility of the contractor. It does not necessarily express the views of the U.S. Geological Survey.

Airborne Gamma-Ray Spectrometer
and
Magnetometer Survey
San Juan Mountains, Colorado
July 16, 1980

Prepared by:

High Life Helicopters Inc./QEB Inc.

Prepared for:

The United States Geological Survey

TABLE OF CONTENTS

FIGURES

FIGURE 1:

Schematic Diagram of Geophysical Sensor System

FIGURE 2:

Data Processing Flow Chart

SUMMARY

High Life Helicopters, Inc., and its subsidiary QEB, Inc., conducted an airborne high-sensitivity radiometric and aeromagnetic survey of the San Juan Mountains area of Colorado for the United States Geological Survey. A LAMA helicopter equipped with a gamma-ray spectrometer and a proton-precession magnetometer collected the data. The gamma-ray spectrometer has a total of 2368 cubic inches of sodium iodide crystal detectors (2048 cubic inches downward-looking and 320 inches upward-looking). The magnetometer has a sensitivity of 0.25 gammas. Visual techniques were used for the navigation and flight-path film was obtained for subsequent position recovery.

Key steps in the data processing were: the correction of the raw radiometric data for altitude dependence (common level reference), cosmic or Compton scatter, atmospheric radon (Bi-air); and the removal of diurnal variations in earth's magnetic field. Products of the data processing consist of magnetic tapes containing raw field data, and single record data; stacked corrected profiles of all radiometric data (Bi-air, total count, potassium, uranium, thorium, eU/eTh, eU/K, eTh/K), magnetic data, radar data; contour maps for uranium, eU/eTH and total magnetic field data.

Due to the substantial relief of the survey area, many of the radiometric sources were located above the NaI detectors carried on the helicopter. This invalidates the assumptions used in deriving the Bi-air corrections (see CALIBRATION RESULTS). For this reason, the Bi-air corrections were computed but not applied to the Uranium channel data.

SYSTEMS

AIRCRAFT

The aircraft used to carry the gamma-ray spectrometer, the magnetometer, and associated electronic equipment was an Aerospatiale SA 315 B LAMA helicopter, Registration No: N49537. It is manufactured in France by Societe National Industrielle, and is designed to haul heavy loads in rugged terrain. Since it operates economically and safely under the most stringent requirements, the LAMA is an ideal aircraft for gamma-ray spectrometer surveys, which must be conducted with heavy payloads, at low speed and at low altitudes.

The LAMA is powered by an 870·SHP Turbomeca Antousti IIIB turboshaft engine, fueled from a 151.3 U.S. gallon (573 liter) fuel tank mounted in the center section of the fuselage. The main rotor is driven through a planetary gearbox with provision for freewheel on autorotation. A take-off drive for the tail rotor is mounted at the lower end of the main gearbox, and a torque shaft connects the latter to a small gearbox which houses the pitch control mechanism, and on which the tail rotor is mounted. Cyclic and collective pitch are power-controlled. Rotors consist of a three-blade main rotor and an antitorque rotor. The main blades are all-metal, are of constant chord, have hydraulic drag-hinge dampers, and are mounted on articulated hinges.

The light metal framework cabin is glazed, while the center and rear of the fuselage behind the cabin have an open triangular framework. The cabin seats a pilot and one passenger side by side and three more passengers behind the pilot. The landing gear is made up of skids with removable wheels. Provision is also made for pneumatic floats for operation on water, and for inflatable emergency flotation gear. The aircraft can carry crystal packs weighing up to 2,204 lbs (1,000 Kg) mounted on external slings. The LAMA is a versatile aircraft which can be adapted for use in rescue operations, liason duties, training, agriculture, and

aerial photography. External dimensions, performance and weight specifications are listed below.

EXTERNAL DIMENSIONS

Main Rotor diameter	36' 1-3/4"
Tail Rotor diameter	6' 3-1/4"
Main Rotor Blade chord (constant)	13.8"
Length overall both rotors turning	42' 4-3/4"
Length of fuselage	33' 8"
Height overall	10' 1-3/4"
Skid track	7' 9-3/4"

GENERAL PERFORMANCE SPECIFICATIONS
BASED ON SEA LEVEL STANDARD CONDITIONS

		Internal		External	
		Average	Maximum	Average	Maximum
At Gross Weight	lb	3,310	4,300	4,200	5,070
Empty Weight	lb	2,216	2,216	2,216	2,216
Useful Load	lb	1,094	2,084	1,984	2,854
Sling Load (max)	lb	-	-	-	2,500
Cruise Speed	mph	118	-	55	75
Top Speed, Vne	mph	-	130	-	-
Useable Fuel US	gal	146	146	46	46
Service Ceiling	ft	(23,000)	17,710	18,370	10,800
HIGE Ceiling	ft	(23,000)	16,730	17,600	9,220
HOGE Ceiling	ft	(23,000)	15,170	16,100	5,000

WEIGHT SPECIFICATIONS FOR GEOPHYSICAL SURVEYS

	Weight (pounds)
LAMA empty weight	2216
Maximum useable fuel	900
Sensor Electronics	850
Pilot	160
Navigator	160
Total	4286

SENSOR ELECTRONICS

A summary of the principle components of the airborne geophysical sensor system - Geodata Model 9600 Airborne radiometric and magnetic system- (shown schematically in Figure 1) - is presented below:

Main Sensors

1. Geodata Model 9600 Airborne Radiometric System.
2. Crystal Detectors - consisting of ten (10) sodium iodide crystals manufactured by Harshaw Chemical Co., Solon, Ohio. These are arranged in two packs with each pack containing four (4) 256 in^3 downward-looking crystals and one (1) 160 in^3 upward-looking crystal. The packs are mounted on the underside of the aircraft on bomb-shackles fitted with a quick release mechanism.
3. Magnetometer - Geometrics Model G-803 with a 0.25 gamma sensitivity.

Ancillary Equipment

1. Radar Altimeter - Collins ALT - 50.
2. Barometric Altimeter - Sensotec Pressure Transducer.
3. Recording Temperature Transducer.
4. Tracking Camera - Automax 35mm Framing Camera (Automax Industries, Woodland Hills, California.

Control Module

1. LSI - II microcomputer (Digital Equipment Corporation) - basic system control.
2. Digital gain stabilizer, multiplexer, time base, high speed A to D and DMA Interface (Geodata International) to monitor and control count rates.

Recording Equipment

1. Pertec 9 track digital tape deck recording at 800 bpi. A Xebec Model XTF - 90 tape controller is used to interface with the LSI - II. The system records:

    a) 512 channels of gamma-ray spectrometer data (256 & 256),
    b) total magnetic intensity,
    c) fiducial number from data system and camera,
    d) altitude from radar and barometric altimeter,
    e) time (days, hours, minutes, seconds),
    f) outside temperature,
    g) "label" information - date, survey area, and flight line number.

2. Digi-Tech analog recorder.

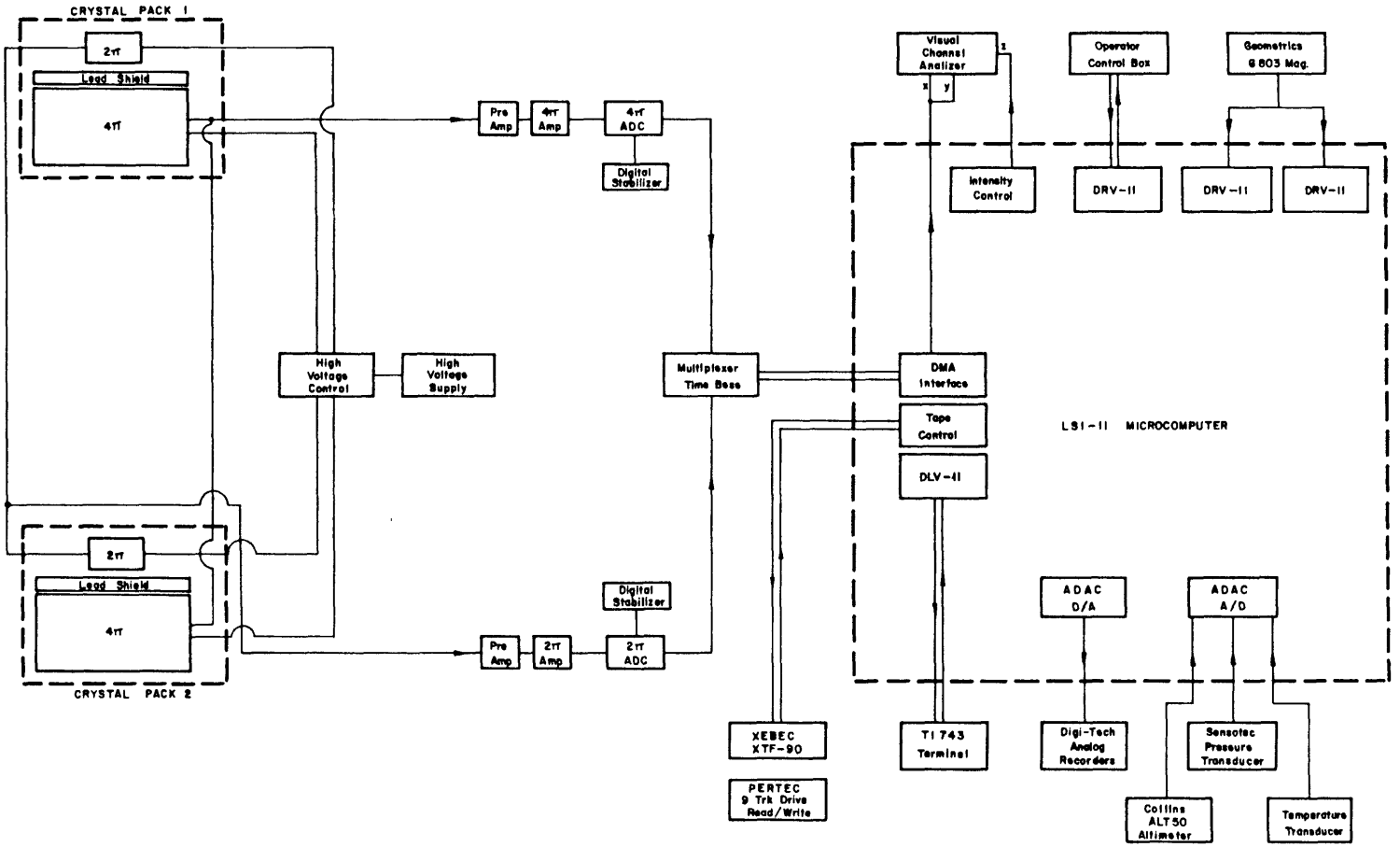

High Life Hellcopters, Inc. / QEB Inc.

System Block Diagram

Lama Hellcopter N 49537

FIGURE 1

COMPUTER FACILITY

QEB uses a remote terminal connection to Information Systems Design, Inc., a computer service organization in Santa Clara, California, A Harris Cope 1620 Modem is used to communicate with a UNIVAC 1108 system.

The UNIVAC 1108 is the hub of ISD's computer service complex. This large scale, drum-oriented system combines high speed batch processing with remote capabilities.

The 1108 central processor has a 65,536 36-bit word ferrite core memory with a 750-NANOSECOND cycle time which uses a corebank overlap feature to give an effective 375-NANOSECOND cycle during program execution. In addition to the main core memory, there are 128 intergrated circuit registers with 125-NANOSECOND cycle time providing multiple accumulators, index registers, I/O access control registers, and special-use registers. A repertoire of over 120 instructions, a real time clock, floating point and double precision hardware, and 16 general purpose I/O channels are the other main feature of this processor.

The 1108 was used exclusively in processing this survey. Other peripheral equipment used in the processing of these data, include:

a) Calcomp 936 Drum Plotter (34" plot width),

b) Calcomp 915 Plotter Controller.

The Calcomp 936 Drum Plotter can be operated either remotely from the ISD facility or locally at QEB from the Calcomp 915 Plotter Controller. The latter is a programmable device consisting of a central processing unit (CPU), a memory unit, a read-write magnetic tape cartridge unit, and a read-only magnetic tape unit (MTU). The 915 can accommodate as many as five peripheral input/output devices on line.

At QEB the MTU reads a data tape created by the 1108 computer. The CPU and a system program read into memory from a tape cartridge then convert the data on the tape into commands that drive an output device.

DATA ACQUISITION

PRODUCTION SUMMARY

Data collection was begun October 4, 1979 near Durango, Colorado and continued through October 8, 1979. North-South traverse lines were flown at a spacing of one-third mile; East-West tie lines (4) were flown at a spacing of four miles. This survey encompassed a total of 786 line-miles of data on twelve 7.5 minute USGS topographic map sheets.

Following is a summary of the daily recording and test results:

Day	Line-Miles Flown	(Cs Equiv.) Average Resolution%	Test-Line Equivalency%
October 4.	278	9.1	5.
October 5.	228	9.1	4
October 6.	123	9.1	4
October 8.	157	9.0	2
Total	786 line-miles		

DAILY SYSTEM CALIBRATION

Pre-flight Checks

a) Cesium sources were positioned at the same point on both the 4π and 2π detector crystals each day to peak each photomultiplier tube. The oscilloscope display and LSI-II microcomputer output indicated the optimum peak setting.

b) The full cesium spectrum was displayed on the CRT for both the upward-looking and downward-looking crystals to calculate the cesium resolution.

c). Thorium sources were used to verify the high energy end of the spectrum for the upward-looking and downward-looking crystals. The output is again displayed on the oscilloscope and/or the LSI-II.

d) The full thorium spectrum for the downward-looking crystals was displayed to verify the location of the K_{40} and Th photopeaks.

In-flight Checks

a) Each day, prior to production flying, a test line approximately 5 miles in length was flown at the planned survey altitude. Data from the test lines were examined to ensure $\pm$ 20% repeatability on total radiometric counts.

Note: The same test line was used each day.

b) During production flying, the visual display units were carefully monitored for changes in the data quality.

c) At the end of each day's production flying, the same test line was re-flown at survey altitude to ensure $\pm$ 20% repeatability of the total radiometric counts.

Post-flight Checks

All pre-flight checks were repeated at the end of the day.

TABLE I - DETECTOR SHIELDING
(UP CRYSTALS)

PHOTOPEAK	PAD	DETECTOR SHIELDING
K	2	= 70.74%

PHOTOPEAK	PAD	DETECTOR SHIELDING
U	4	= 73.19%
Th	3	= 71.20%

TABLE II - SPECTRAL WINDOWS
(APPLIES TO BOTH UP & DOWN CRYSTALS)

K_{40}	(1.361 MEV - 1.561 MEV)
Bi_{214}	(1.659 MEV - 1.871 MEV)
Th_{208}	(2.414 MEV - 2.814 MEV)
COSMIC	(3.000 MEV - 6.000 MEV)
TOTAL	(0.400 MEV - 3.000 MEV)*

*Nominal value - Exact value of upper energy cut off depends upon E_o and $\Delta E/\Delta CH$. Average value at Walker Field - 3.000 MEV

FLIGHT PATH RECOVERY

Navigation was by visual identification of prominent ground features. During each flight, films were taken of the flight path. At the end of each flight these films were developed and used to correlate with the USGS topographic sheets. The final pick points were then located on 1:24,000 topographic map sheets (12 in this area).

DATA PROCESSING FLOW CHART
(USGS)

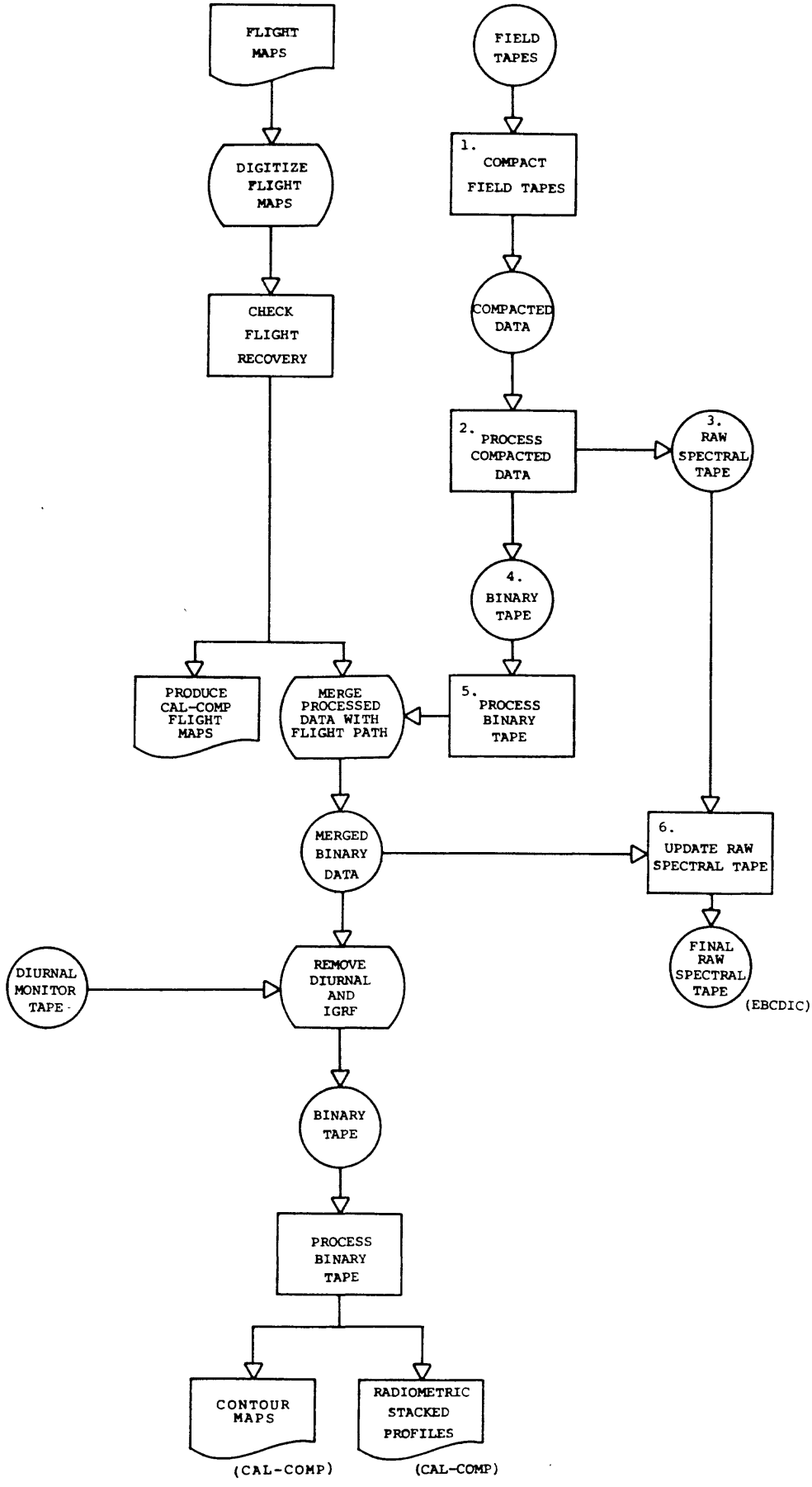

FIGURE 2

DATA PROCESSING

PRE - PROCESSING

By "pre - processing", we refer to those procedures that are applied to the field data and flight line locations to prepare them for final processing, merging, and output.

Steps in this "pre-processing" stage include field data tape editing and compacting, flight line location verification, and generation of preliminary data reports. The reader is referred to the data processing flow chart, Figure 2 which accompanies this report, and which illustrates the steps described below.

Field Tape Compacting and Editing

A check of the field data tapes by computer is necessary to verify data collection and recording quality. The summed spectral data for both 4π and 2π crystals are first read from a series of merged field tapes. The centroids of channel photopeaks for each flight line are next calculated from these data and linear equation which relates the photo energy (in MeV) to the channel number is derived from the centroid calculation. This equation is of the form

$$E = E(0) + \partial E/\partial ch \times ch$$

where $E(0)$ is the apparent energy at channel zero, ch is the channel number (0-255). This procedure is not applied if the survey line is too short (less than 10 minutes time duration) to establish adequately smooth summed spectral data for photopeak centroid location. In the event of too short a survey line, data from other lines are "stacked" to achieve adequate statistics for photopeak calculations. Next, the summed or "stacked" spectral data are used to calculate the resolution for K, U and Th photopeaks. Both photopeak linearity and resolution are used to establish the acceptability of the spectrometer data.

Next, the data within each flight line were checked for correct one (1) second and ten (10) second scan lengths. Erroneous scan lengths are flagged, and the spectral data for the erroneous scans are not used in the subsequent data analysis. The data from each scan are used to extract one second channel window data fields. These data fields are corrected for system "dead time"

at this stage.

At termination of this stage of the data processing, two computer tapes are written (item 3 and 4 of Figure 2).

Item 3 is a partially written RAW SPECTRAL TAPE containing all of the required data entries exclusive of the location information.

Item 4 is a tape written in internal UNIVAC 1108 binary code. This tape contains all of the required data entries for further processing. Full spectral data are not written on this tape, as these are contained on the partial RAW SPECTRAL TAPE.

Editing is next performed on the binary tape. Further checking consists of re-reading (with unnecessary flight data removed); and searching for and removing unrealistic gradients, transients, spikes etc. The acceptability of questionable data segments is reviewed and corrections performed. The result of this procedure is an edited tape, which has "clean data" available for step 5 of the data processing (figure 2).

Flight Line Recovery

Determining actual flight-line location is a crucial task in the data processing. It is accomplished primarily by using photographs taken in flight. After the flight film is developed, a photo interpreter correlates the photo-data with the flight navigator's visual location picks on the NTMS map sheets. Actual aircraft locations are determined from the flight films and transferred to the base map with the fiducial numbers of the corresponding photographs.

Once data transfer to the base map is complete, fiducial numbers and locations along each flight line are digitized, and an automated computer routine checks the consistency of these data. This is done by calculating the average distance between fiducials, and establishing that this distance varies reasonably along a given flight line,

After computer verification, map coordinates for each photopick point of each flight line are calculated and a computer plot of these points made and checked against the field plot. Any discrepancies are noted, and the misplaced pick points are relocated from the flight film. The procedure is repeated until internal consistency is achieved.

Once the flight line data are verified, a mylar transparency of the flight lines is then prepared on the Cal Comp 915, at a scale of 1:24,000.

RADIOMETRIC DATA PROCESSING

The "cleaned" data require a number of corrections before data plots can be produced. These are done in step 5 (Figure 2) and include:

1. Aircraft and cosmic background correction.
2. Compton stripping.
3. Radon correction.
4. Altitude correction.

These corrections are discussed in more detail in the section entitled "CALIBRATION RESULTS". After these corrections are made, these processed data are merged with the flight path data.

MAGNETIC DATA PROCESSING

Steps in the reduction of the magnetic data consist of corrections for diurnal variations, and common magnetic datum tieing. A ground based magnetometer monitored diurnal variations of the magnetic field during the airborne operation. Data were sampled at 4 second intervals at a sensitivity of one quarter gamma was recorded along with time code on analogue tapes. Editing was performed to remove data spikes, man-made magnetic events and extraneous reading. A profile display was made as a check to determine visually that all necessary editing had been performed. The edited, compacted diurnal data are time coded to match the airborne data, (see Figure 2) densified to a one (1) second sample interval and subtracted from the airborne data.

Magnetic differences in the resultant diurnally corrected plots between tie lines and flight lines at intersections are treated by a tieing program. Individual line biases are calculated for both

tie and profile lines. These biases are caused by changes of ground based magnetometer location, aircraft magnetization, and effects due to differential aircraft heading.

The diurnal corrections and the calculated biases are then applied to the merged binary tape (Step 7, Figure 1). This now completes the data processing stage of the analysis. Data on the merged binary tape is now ready for display and final presentation.

DATA DISPLAY

Data and information derived from this project are displayed in a number of formats. These formats are flight path location maps, stacked profiles, and contour maps of U, U/T ratio and total field magnetics. A single record reduced data tape was submitted under separate cover.

FLIGHT PATH LOCATION MAPS

The actual flight path position for each flight line and tie line, as utilized in data analysis, is displayed for each NTMS quadrangle of the project. Topographic quadrangle maps at a scale of 1:24,000 are utilized as the base map for superpositioning of flight lines. Ancillary information consisting of flight and tie line number and fiducial number of located positions is also printed on these maps.

STACKED PROFILES

The stacked profiles consist of: (1) corrected Total Count, (2) corrected Potassium 40 in percent, (3) corrected Bi 214 in equivalent U ppm, (4) corrected TI 208 in equivalent ppm, (5) uranium/thorium ratio, (6) uranium/potassium ratio, (7) thorium/uranium ratio, (8) Bi-Air, (9) radar altimeter, (10) magnetometer data. Plotted at a linear scale of 1:24,000, these profiles are representative of processed data along a given flight line within the confines of a specific NTMS sheet. As such these can be directly superimposed on the

flight path maps, topographic maps, etc., at a scale of 1:24,000

CONTOUR MAPS

Contour maps were created and plotted automatically for Bi-214 (in ppm), Bi-214/TI208 ratio, and total magnetic field (in gammas). The method of creating the maps is to first determine the values at the corners of a grid cell for each variable. In this area, the grid cells were squares 150 meters on each side; fine grid cells were used to preserve local anomalies. Smoothed contours were then created by another computer program to connect areas with equal values.

All of the aforementioned output products were submitted to the U.S.G.S. previously under separate cover.

CALIBRATION RESULTS

1. Aircraft and Cosmic Background

Background effects due to the natural radioactivity of the aircraft frame and all of the equipment were calculated from a series of high-altitude sorties (from 3,000 - 12,000 feet) over the Pacific Ocean. In this process, a cosmic correction ratio is also determined which is a dimensionless factor to eliminate contributions from cosmic energies within each channel.

A general matrix equation can be written for the measured count rate (for high altitude flights):

$$Y = C \cdot X + BG$$

where,

(known) Y = measured count rate (in each channel) at each altitude (a function of altitude)

(known) X = measured cosmic count rate at each altitude (a function of altitude)

(unknown) C = cosmic correction ratio (in each channel)

(unknown) BG = background effect (in each channel)

The cosmic correction ratios and backgrounds were determined by least squares analysis of the channel data over the suite of (5) altitudes.

Aircraft and cosmic background for the LAMA over the channel windows as derived from these flights are listed below:

AIRCRAFT AND COSMIC BACKGROUNDS - N-49537

4 - 27 - 79

CHANNEL WINDOW	AIRCRAFT BACKGROUND COUNTS/SEC	COSMIC CORRECTION RATIO (DIMENSIONLESS)
K40 (4π)	6.02	.2092
Bi214 (4π)	2.52	.1825
Th208 (4π)	2.37	.2176
TOTAL COUNT	64.68	3.4579
Bi214 (2π)	0.62	.2143

2. COMPTON STRIPPING:

WALKER FIELD DATA COLLECTION PROCEDURES

Full spectral data were measured and digitally recorded above each of the five calibration pads at the Walker Field facility. Data were collected over each pad during a five minute time interval. A sample rate of one full scan (256 channels down crystal - 256 channels up crystal) per second gave a total of 300 spectral measurements per calibration pad.

Each of the five pads at the field contains a fixed concentration of potassium, uranium, and thallium. According to Bendix Field Engineering Corporation, these concentrations are given in Table I below:

TABLE I - NOMINAL PAD CONCENTRATION - WALKER FIELD

Pad	K	Th	U
1. (Background)	1.45%	6.26 ppm	2.19 ppm
2. (K)	5.14%	8.48 ppm	5.09 ppm
3. (Th)	2.01%	45.33 ppm	5.14 ppm
4. (U)	2.03%	9.19 ppm	30.29 ppm
5. (Mixed)	4.11%	17.52 ppm	20.39 ppm

In the data analysis, we are concerned with the differential concentrations of Pads 2 through 5 with respect to Pad 1 (Background).

First, the system sensitivities are calculated from a matrix equation of the form:

$$I = RHO \cdot S$$

where,

(known) I = count rate matrix of each channel on each pad

(known) RHO = concentration matrix for each pad and each variable

(unknown) S = matrix of response (or sensitivity) in each channel due to input energy from all channels

This last matrix, S, is the matrix of sensitivities we estimate by least-squares regression.

To calculate the "stripping" coefficients ϕ, we rewrite the previous equation:

$$RHO = S^{-1} \cdot I$$

where,

S^{-1} = the inverse sensitivity matrix

Upon expanding, we have equations of the form:

$$RHO(Eu,j) = S_z{}^{u}I \equiv S_z((^{u}Ij) - {}^{u}\phi TH(^{TH}Ij) - {}^{u}\phi_K(^{K}Ij))$$

(and equivalent equations for each channel)

where,

Eu = 1.76 MEV (Bi-214 Photopeak)

uIj = count rate of U channel on pad j

^{TH}Ij = count rate of TH channel on pad j

^{K}Ij = count rate of K channel on pad j

j = 2,5

${}^{u}\phi Th$ = effect of energy from Th channel on U channel

${}^{u}\phi K$ = effect of energy from K channel on U channel

etc.

Since there are six of these unknown stripping coefficients and 12 equations (4 pads , 3 channels each) we can again solve for the best answers by least-squares regression.

The results from these analyses are tabulated below in Tables II, III, IV:

SENSITIVITY COEFFICIENTS AND STRIPPING RATIOS

TABLE II - DERIVED SYSTEM SENSITIVITIES
(DOWN CRYSTALS)

K_3 = 223.31 CPS/%K

K_2 = 21.99 CPS/PPM eU

K_1 = 11.31 CPS/PPM eTh

TABLE III - DERIVED SYSTEM "STRIPPING" COEFFICIENTS
(DOWN CRYSTALS)

$K_{\phi U} = 0.835219$

$K_{\phi Th} = 0.089280$

$U_{\phi Th} = 0.354857$

$U_{\phi K} = 0.055247$

$Th_{\phi U} = 0.130138$

$Th_{\phi K} = 0.0$

TABLE IV - COMPARISON OF ACTUAL AND DIFFERENTIAL PAD CONCENTRATIONS

PAD		%K	PPM U	PPM Th
2 (K)	Calc.	3.64	3.12	2.08
	Actual	3.69	2.90	2.22
3 (Th)	Calc.	.47	3.37	39.62
	Actual	.56	2.95	39.07
4 (U)	Calc.	.51	28.77	3.72
	Actual	.58	28.10	2.93
5 (MIXED)	Calc.	2.39	19.39	12.84
	Actual	2.66	18.20	11.26

3. RADON CORRECTION

The Bi Air (Radon) contribution to the counts measured in the 4π bismuth channel are approximated by:

$$Bi_A = \frac{U_{UP} - Bo(Z_{STP}) * U_L' - C_o T_L}{\phi_B(Z_{STP}) - B_o(Z_{STP})}$$

where:

U_{UP} = Count Rates in Bi channel from 2π detector

U_L' = Compton Scatter corrected Bi count rate (4π detector)

T_L = Compton Scatter corrected Th count rate (4π detector)

$\phi_B(Z)$ = 4π to 2π geometric ratio (height dependent)

$B_o(Z)$ = 4π to 2π bismuth coupling factor (height dependent)

C_o = 4π to 2π thallium coupling factor (constant)

Values for these factors were established at the Lake Mead Dynamic Test Range and the Walker Field Test Facility.

$$B_o(Z) = 0.045894 - .000064 \times Z$$

$$\phi_B = 0.21727 - .00006359 \times Z_{STP}$$

$$C_o = 0.023331$$

LAKE MEAD CALIBRATION

This section of the report describes the calibration on May 3, 1979, of LAMA Helicopter N-49537 at the Lake Mead Dynamic Test Range, Las Vegas, Nevada. During the data collection, weather was clear with winds from the north at 10 mph. Surface temperatures varied from 22-31°C during the data sorties.

4. ALTITUDE ATTENUATION COEFFICIENTS

$$\mu_{TC} = -.0020586\ F + {}^{-1}$$

$$\mu_{K} = -.0026287\ F + {}^{-1}$$

$$\mu_{U} = -.0024875\ F + {}^{-1}$$

$$\mu_{T} = -.0020933\ F + {}^{-1}$$

These coefficients were determined by least squares fitting of the stripped, low-altitude data at Lake Mead and are employed to reduce the measured count rate at any elevation to 400 feet (at STP of $0^{o}C$ - 760 mm Hg). The reduction formula is given by:

$$\text{COUNTS NORMALIZED} = \text{COUNTS MEASURED} * \text{EXP}\ (+\mu i * (Z_{STP} - 400))$$

$$Z_{STP} = Z_{MEAS.} \frac{*P*273.15}{760*(273.15+T)}$$

where:

μ_i is the channel attenuation constant

P is the measured atmospheric pressure (mm of Hg)

T is the temperature in degrees Celsius

The reduction to STP is necessitated to correct for air density changes along the ground-detector optical path.

The preceding pages have summarized the necessary corrections to the radiometric data.

4. TOPOGRAPHIC EFFECTS

The Bismuth coupling factor $B_O(\bar{z})$ computed from the LAKE MEAD data, is derived from sources below the 4π and 2π crystal detector array. When radiometric sources are above the detector package, as occurs for example in canyons, below ridge lines, and within cirques, the coupling terms are modified by the appreciable shielding effects of the 2π detector.

No calibration facilities exist for determination of the coupling-shielding effects due to sources above the detector array. Due to the complexity of topography and the lack of data to establish the solid angle responce of the detector system, it was not possible to mathematically estimate these source effects. Thus the Bi-air correction formula given in section 3 was not applied to the 4 Bismuth channel data. This formula was used to compute an "apparent Bi-air correction" which is presumably valid in those areas of the survey where topography is not extreme.